

From source to target and back: symmetric bi-directional adaptive GAN

P. Russo, F. M. Carlucci, T. Tommasi, and B. Caputo

Department of Computer, Control, and Management Engineering Antonio Ruberti

Sapienza University of Rome, Italy

{ prusso,fabio.m.carlucci,tommasi,caputo } @dis.uniroma1.it

May 4, 2022

Abstract

The effectiveness of generative adversarial approaches in producing images according to a specific style or visual domain has recently opened new directions to solve the unsupervised domain adaptation problem. It has been shown that source labeled images can be modified to mimic target samples making it possible to train directly a classifier in the target domain, despite the original lack of annotated data. Inverse mappings from the target to the source domain have also been evaluated but only passing through adapted feature spaces, thus without new image generation.

In this paper we propose to better exploit the potential of generative adversarial networks for adaptation by introducing a novel symmetric mapping among domains. We jointly optimize bi-directional image transformations combining them with target self-labeling. Moreover we define a new class consistency loss that aligns the generators in the two directions imposing to conserve the class identity of an image passing through both domain mappings.

A detailed qualitative and quantitative analysis of the reconstructed images confirm the power of our approach. By integrating the two domain specific classifiers obtained with our bi-directional network we exceed previous state-of-the-art unsupervised adaptation results on four different benchmark datasets.

1 Introduction

The ability to generalize across domains is crucial for visual recognition systems deployed in the wild. This is especially challenging when there is ample labeled data on which to train a deep network (source domain), but no annotated data where eventually the trained model should be used (target domain). To attack this issue, research in domain adaptation has proposed a wide array of methods over the last years, most of them aiming at reducing the shift among the source and target distributions (for a review of previous work we refer to section 2). One alternative adaptive technique consists in mapping the source data into the target domain: this can be obtained either by modifying the image representation [8] or by directly generating a new version of the source images [2]. Several authors proposed approaches that follow both these strategies by building over the recent and ongoing success of Generative Adversarial Networks (GAN) [11]. A similar but inverse method consists in mapping the target data into the source domain, where there is already abundance of labeled images [28].

We argue that these two mapping directions should not be seen as alternative, but as complementary. Indeed, the main ingredient for adaptation is the ability of transferring successfully the style of one domain to the images of the other. This, given a fixed generative architecture, will heavily depend on the application: there may be cases where mapping from the source to the target is easier, and cases where it is true otherwise. We argue that by pursuing both directions in a unified architecture, we can obtain a system more robust and more general than previous adaptation algorithms.

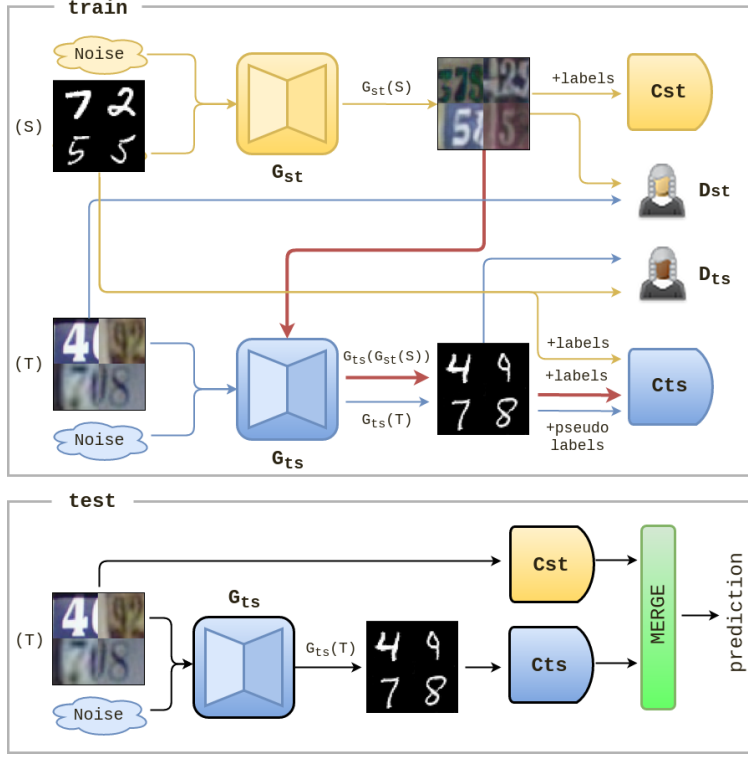


Figure 1: Schematic illustration of our SBADA-GAN. In the training phase, yellow lines represent data flow from source to target, while blue lines represent data flow from target to source. The red lines indicate the proposed *class consistency* condition that constraints a source image to keep its own label when passing sequentially through the two generators G_{st} and G_{ts} for domain transformations. During test phase the target samples are fed directly to C_{st} and transformed by G_{ts} before entering C_{ts} , to match the respectively classifiers trained data styles. The output of the two classifiers are merged by linear combination to get the final prediction.

With this idea in mind, we designed SBADA-GAN: Symmetric Bi-Directional ADaptive Generative Adversarial Network, which represents the main contribution of this paper.

Concretely, we start from labeled source samples S and from unlabeled target samples T . Our architecture (see Figure 1 for a schematic overview) exploits two generative adversarial losses that encourage the network to produce $G_{st}(S)$ target-like images from the source samples and $G_{ts}(T)$ source-like images from the target samples. We jointly optimize two classification objective functions, one on the original source images S and the other on the transformed target-like source images $G_{st}(S)$. Moreover, we take advantage of the source annotation in two novel ways: (i) reliable pseudo-labels are automatically assigned to $G_{ts}(T)$ data which then contribute to regularize the classifier trained on S and also improve the same generator model G_{ts} by backpropagation; (ii) we define a new reconstruction constraint on the source images: the *class consistency loss*, imposes that by mapping source images towards the target domain $G_{st}(S)$ and then again towards the source domain ($G_{ts}(G_{st}(S))$) they get back to their ground truth class.

This last condition is less restrictive than a standard reconstruction loss [14], as it deals only with the image annotation and not with the image appearance. Still, it is highly effective in aligning the domain mappings in the two directions. Finally, the classifier trained on S is tested on $G_{ts}(T)$ and the classifier trained on $G_{st}(S)$ is tested on T . Our bi-directional architecture provides realistic image reconstructions and by simple linear combination of the two classifier predictions it exceeds previous state-of-the-art unsupervised adaptation results on four different benchmark datasets.

In the rest of the paper we first review relevant previous work (section 2). We then describe SBADA-GAN (section 3) and then we test it with qualitative and quantitative experiments (section 4). We conclude with a summary and outlining future research directions (section 5).

2 Related Work

GAN Generative Adversarial Networks (GANs) [11] are composed of two modules, a generator and a discriminator. The generator’s objective is to synthesize samples whose distribution closely matches that of real data, while the discriminator objective is to distinguish real from generated samples.

GANs are agnostic with respect to the training samples labels, while the conditional GAN variants [20] exploit the class annotation as additional information to both the generator and the discriminator. Some works have recently tried to use multiple GANs: in CoGAN [17] two generators and two discriminators are coupled by weight-sharing to learn the joint distribution of images in two different domains without using pair-wise data. Both Cycle-GAN [30] and Disco-GAN [14] encourage the mapping between two domains to be well covered by imposing transitivity: the mapping in one direction followed by the mapping in the opposite direction should arrive where it started. This is obtained through consistency conditions based on reconstruction losses. For this image generation process the main performance measure is either a human-based quality control (verify if a human can recognize real images against generated ones) or scores that evaluate the interpretability of the produced images by pre-existing models (e.g. trained for classification [23], segmentation [30], etc.).

Domain Adaptation The presence of a domain shift between train and test data largely reduces the accuracy of existing learning methods due to practical generalization limits. A recent, widely used adaptive strategy consists in minimizing a loss which either measures the errors in target samples reconstruction [10], or measures the difference between source and target distributions [29, 26, 4]. Domain invariance can be also treated as a binary classification problem through an adversarial loss inspired by GANs, which encourages mistakes in domain prediction [8]. For all these methods, the described losses are minimized jointly with the main classification objective function on the source task, with the aim of guiding the feature learning process towards a domain invariant representation. Only in [28] the two objectives are kept separated and recombined in a second step. Here the authors still exploit an adversarial loss, but the goal is to optimize the target feature mapping to match the source, rather than the other way round. Finally, the source classifier is used on the modified target. An alternative solution has been proposed in [3]. Here the feature components that explicitly separate the domains are modeled separately from the feature shared among the domains. This goal is obtained through a reconstruction loss for each domain, a similarity loss that encourages domain invariance, and a difference loss that encourages the common and private representation component to be complementary.

Image Generation for Domain Adaptation In the first style transfer methods [9, 13] new images were synthesized to maintain a specific content and replicating the style of one or a set of reference images. Similar transfer approaches has then be used to generate images with different visual domains. In [25] realistic samples were generated from synthetic images and it has been shown that the produced data could work as training set for a classification model with good results on real images. [2] proposed a GAN-based approach that adapts source images to appear as if drawn from the target domain and the classifier trained on the newly produced data outperform several domain adaptation methods by large margins. [27] introduced a method to generate source images that resemble the target ones, with the extra consistency constraint that the same transformation should keep the target samples identical. All these methods focus on the source to target image generation. They do not consider the possibility of an inverse procedure, leading from target to source, and the benefit that this solution could bring in combination with the standard source-to-target direction.

3 Method

Model We focus on unsupervised cross domain image classification. Given data drawn from a labeled source domain $S = \{x_s, y_s\}$ and from a different unlabeled target domain $T = \{x_t\}$ belonging to the same set of categories, the task is to maximize the classification accuracy on T while training on S . To reduce the domain gap, we propose to adapt the source images such that they appear as sampled from the target domain by training a generator model G_{st} that maps the source samples x_s and a noise vector z to target-like images $x_{st} = G_{st}(x_s)$. The model is also augmented with a discriminator D_{st} and a classifier C_{st} . The former takes as input both target images x_t and source transformed images x_{st} , learning to recognize them as belonging to two different sets. The latter takes as input the transformed images x_{st} and learns to assign the task-specific labels y_s to each sample. During the training procedure for this model, information about the domain recognition likelihood produced by D_{st} is used adversarially to guide and optimize the performance of the generator G_{st} . Similarly, the generator also benefit of backpropagation from the classifier training procedure.

Besides the source-to-target transformation, we also consider the inverse target-to-source direction by using a symmetric architecture. Here target images x_t and a noise vector z are given as input to a generator model G_{ts} mapping them to source-like images $x_{ts} = G_{ts}(x_t)$. As before, the model is augmented with a discriminator D_{ts} which takes as input both x_{ts} and x_s and learns to recognize them as belonging to two different sets, adversarially helping the generator. Here, since the target images are unlabeled, apparently no classifier can be trained as a further support for the generator model. We overcome this issue by *self-labelling*. The original source images x_s and their ground truth labels y_s are used to train a classifier C_{ts} . Given the abundance of the source samples, this classifier tends to achieve high performance after a short training period. Once it has reached convergence, we use the learned model to annotate the modified target images x_{ts} . These samples, with the assigned pseudo-labels, are then used transductively as input to C_{ts} while information about the performance of the model on them is backpropagated to guide and improve the generator G_{ts} .

Finally, the symmetry in the source to target and target to source transformations is enhanced by aligning the two generator models such that when used in sequence they bring a sample back to its starting point. Since our main focus is classification, we are interested in preserving the class identity of each sample rather than its overall appearance. Thus, instead of a standard image-based reconstruction condition we introduce a class-based reconstruction condition. Specifically, we impose that a source image x_s adapted to the target domain through $G_{st}(x_s)$ and transformed back towards the source domain through $G_{ts}(G_{st}(x_s))$ is correctly classified by C_{ts} . This condition helps by imposing a further joint optimization of the two generators. An overall view of the described adversarial model can be seen in figure 1.

Learning Here we formalize the description of the previous section by providing more details about the model parameters and the objective functions optimized while training our SBADA-GAN architecture. Let us start by fully defining the generators $G_{st}(x_s, z; \theta_{G_{st}})$, $G_{ts}(x_t, z; \theta_{G_{ts}})$, as well as the discriminators $D_{st}(x; \theta_{D_{st}})$, $D_{ts}(x; \theta_{D_{ts}})$ and the classifiers $C_{st}(x; \theta_{C_{st}})$, $C_{ts}(x; \theta_{C_{ts}})$.

The direct source-to-target part of the network optimizes the following objective function:

$$\min_{\theta_{G_{st}}, \theta_{C_{st}}} \max_{\theta_{D_{st}}} \alpha L_{D_{st}}(D_{st}, G_{st}) + \beta L_{C_{st}}(G_{st}, C_{st}) , \quad (1)$$

where the classification loss $L_{C_{st}}$ is a standard *softmax cross-entropy* evaluated on the source samples transformed by the generator G_{st} :

$$L_{C_{st}}(G_{st}, C_{st}) = E_{\{x_s, y_s\} \in S, z} [-y_s^\top \log(C_{st}(G_{st}(x_s, z; \theta_{G_{st}}); \theta_{C_{st}}))] , \quad (2)$$

while we followed [19] and chose a *least square* loss for the discriminator instead of the less robust binary cross-entropy:

$$L_{D_{st}}(D_{st}, G_{st}) = E_{x_t \in T} [(D_{st}(x_t; \theta_{D_{st}}) - 1)^2] + E_{x_s \in S, z} [(D_{st}(G_{st}(x_s, z; \theta_{G_{st}})))^2] . \quad (3)$$

For the inverse target-to-source part of the network the objective function to optimize is:

$$\min_{\theta_{G_{ts}}, \theta_{C_{ts}}} \max_{\theta_{D_{ts}}} \gamma L_{D_{ts}}(D_{ts}, G_{ts}) + \mu L_{C_{ts}}(C_{ts}) + \eta L_{C_{ts}}(G_{ts}, C_{ts}) , \quad (4)$$

where the first classification loss is a standard *softmax cross-entropy* evaluated on the original source samples, thus it neither has any dependence on the generator that transforms the target samples G_{ts} , nor it provides feedback to it:

$$L_{C_{ts}}(C_{ts}) = E_{\{x_s, y_s\} \in S} [-y_s^\top \log (C_{ts}(x_s; \theta_{C_{ts}}))] . \quad (5)$$

The second classification loss is again a *softmax cross-entropy* but it deals with the *self-labeled* target samples and back-propagates to the generator G_{ts} such that it is encouraged to preserve the annotated category within the transformation:

$$L_{C_{ts}}(G_{ts}, C_{ts}) = E_{\{x_t, y_{t_{self}}\} \in T, z} [-y_{t_{self}}^\top \log (C_{ts}(G_{ts}(x_t, z; \theta_{G_{ts}}); \theta_{C_{ts}}))] . \quad (6)$$

Finally, we developed a novel *class consistency* loss by minimizing the error of the classifier C_{ts} when applied on the concatenated transformation $G_{ts}(G_{st}(x_s))$ with the corresponding ground truth label y_s :

$$L_{C_{ts}}(G_{ts}, G_{st}, C_{ts}) = E_{\{x_s, y_s\} \in S, z_s, z_t} [-y_s^\top \log (C_{ts}(G_{ts}((G_{st}(x_s, z_s; \theta_{G_{st}}), z_t; \theta_{G_{ts}}); \theta_{C_{ts}}))] \quad (7)$$

This loss has the important role of aligning the generators in the two directions and strongly connecting the two main parts of our architecture. An evidence of its crucial effect can be observed in Figure 2, where we show the comparison with the images produced by the generator G_{ts} when either no consistency condition is applied on $G_{ts}(G_{st}(x_s))$, or the image-based reconstruction condition is applied through the *cycle consistency* loss presented in [30, 14]. Our class consistency loss allows to preserve the distinct features belonging to a category while still leaving enough freedom to the generation process. On the contrary, the image-based reconstruction losses tend to preserve too many input structure, or they does not allow at all any modification of the image.

By collecting all the presented parts, we conclude with the complete SBADA-GAN objective function:

$$\begin{aligned} L_{SBADA-GAN}(G_{st}, G_{ts}, C_{st}, C_{ts}) = \\ \min_{\theta_{G_{st}}, \theta_{G_{ts}}, \theta_{C_{st}}, \theta_{C_{ts}}} \max_{\theta_{D_{st}}, \theta_{D_{ts}}} \alpha L_{D_{st}}(D_{st}, G_{st}) + \beta L_{C_{st}}(G_{st}, C_{st}) + \\ \gamma L_{D_{ts}}(D_{ts}, G_{ts}) + \mu L_{C_{ts}}(C_{ts}) + \eta L_{C_{ts}}(G_{ts}, C_{ts}) + \\ \nu L_{C_{ts}}(G_{ts}, G_{st}, C_{ts}) . \end{aligned}$$

Testing The classifier C_{st} is trained on $G_{st}(x_s)$ generated images that mimic the target domain style, and is then tested directly on the original target samples x_t . The classifier C_{ts} is trained directly on x_s source data, and then tested on $G_{ts}(x_t)$ samples, that are the target images x_t modified to mimic the source domain style. These classifiers make mistakes of different type assigning also a different confidence rank to each of the possible labels.

Overall the two classification directions complement each other. We take advantage of this with a simple ensemble method which linearly combines their probability output, providing a further gain in performance. We set the combination weights through cross validation (see section 4 for further details).

4 Evaluation

4.1 Datasets and Adaptation Scenarios

To assess SBADA-GAN against previous works, we consider the following widely used digits datasets:

MNIST[16] is an historical dataset proposed by LeCun in 1998. It contains 70.000, 28×28 pixel, grayscale images (of which, 10.000 act as test set). Each sample contains a centered, single digit number between



Figure 2: G_{ts} outputs (lower line) and their respective inputs (upper line) obtained with: (a) no reconstruction loss, (b) image-based cycle consistency loss [30, 14], (c) our label-based class consistency loss. When no reconstruction loss is activated, the G_{ts} output is realistic, but it fails at reproducing the correct input digit, and provides misleading information to the classifier. The cycle-consistency loss preserves the input digit but fails in rendering a realistic sample. Finally, our class consistency loss succeeds in both preserving the digits and rendering a realistic sample. In (d) we show some real svhn samples as a reference.

0 – 9 on a black background. **MNIST-M**[7] is a variant of the *MNIST* dataset where the background is substituted by a randomly extracted patch obtained from color photos from BSDS500[1]. **USPS**[6] is *MNIST* look-a-like, composed by 7291 training and 2007 testing 16×16 pixel grayscale samples, automatically scanned from envelopes by the U.S. Postal Service and then centered and normalized. It presents a broad range of font styles. **SVHN**[21] is a challenging real-world dataset, much larger in scale than the previous ones: it contains over 600.000 32×32 pixel color samples. In addition to presenting a great variety of styles (in shape and texture), samples from this dataset often contain extraneous numbers in addition to the labeled, centered one. Most previous works simplified this dataset by considering a grayscale version: we apply our method to the original RGB images.

Starting from these databases, we consider the following settings, all in the unsupervised scenario (i.e., only the source labels are available during training). **MNIST to MNIST-M**: we follow [3, 2], which use the evaluation protocol of [7] and use 1.000 samples from the target training set for validation purposes. **MNIST to USPS / USPS to MNIST**: we again follow [2] and use 50.000 samples from the MNIST training set and use the standard splits for USPS, comprising of 6.562 training, 729 validation, and 2.007 test images (we resize *USPS* to 28×28 pixels). **SVHN to MNIST / MNIST to SVHN**: we use the protocol by [3, 10] and consider the full training sets, while withholding 1.000 target samples for validation purposes (we resize *MNIST* to 32×32 pixels).

4.2 Implementation details

We ran all our experiments in the Keras framework [5] (code will be made available upon acceptance); all training used the ADAM[15] optimizer. We train all models for 500 epochs not noticing any overfitting, which suggests that further epochs might be beneficial. Learning rates for the discriminator and the generator are both set to 10^{-4} ; batch size is set to 16. The basic setup of SBADA-GAN loss weights are: α and γ (discriminator losses) set to 1.0, β and μ (classifier C_{st} and C_{st} losses) set to 10.0, so to prevent that the generator might indirectly switch labels (for instance, transform 7s into 1s). Class consistency loss weight ν has been set to 1.0. For the *MNIST-MNIST-M* experiment, β is set to 1.0, μ and ν have been set to 0.1 as the strong connection between *MNIST* and *MNIST-M* samples reduces the workload for classification and regularization losses.

Setting	Source	Target mapped to Source	Source mapped to Target	Target
MNIST -> USPS	0.206	0.219	0.106	0.102
MNIST -> MNIST-M	0.206	0.207	0.035	0.032
MNIST -> SVHN	0.206	0.292	0.027	0.012

Table 1: Dataset mean structural similarity index: this measure of data variability suggests that our method successfully captures each domain’s complexity.

All training procedures start with the self-labeling loss weight, λ , set to zero, as this loss hinders convergence until the classifier is fully trained. After the model converges (losses stop oscillating, usually after 250 epochs) λ is set to 1.0 to further increase performances.

Architectures The GAN architecture is the same used by [2] with a residual model for the generator and the standard DCGAN-like model as discriminator. In particular, the generator is made of four residual blocks with the input noise concatenated as five extra channels with the input sample channels. Each residual block has two convolutional layers with 64 features. The discriminator is made of two convolutional layers, followed by an average pooling and a kernel convolution that brings the discriminator output to a single scalar value. The classifier is the very same of [2, 8] to enable a fair comparison, using the same number of neurons [2] w.r.t to a wider fully connected layer of [8]. In both generator and discriminator networks, each convolution (with the exception of the last one of the generator) is followed by a batch norm [12] layer. Note that, thanks to the stability of the SBADA-GAN training protocol, we did not use any injected noise into the discriminators layers and we removed all the dropout layers. We further avoided the trick [2] of training the classifier also on input samples to improve the training stability. As activation functions we used ReLU in the generator and classifier and leaky ReLU (with a 0.2 slope) in the discriminator as a standard GAN setup.

4.3 Qualitative Results

To evaluate the quality of our generated images, we considered: (a) the *TSNE*[18] visualization of different source, target and mapped distribution (fig. 4) in the raw pixel space. We clearly see that the transformed dataset replicates the target distribution appropriately; (b) *SSIM*: we follow [22] (but avoid the multiscale computation, as the images are too small) and compute the structural similarity index (SSIM) for each dataset (table 1). The SSIM between two images is a number which is 1 if the images are identical and goes to 0 the more they are different. By randomly sampling a sufficiently large number of image pairs from each dataset, and averaging the results, we can get a good estimate of the dataset’s image variability. Values in table 1 confirm that we successfully capture the target’s variability.

4.4 Quantitative Results

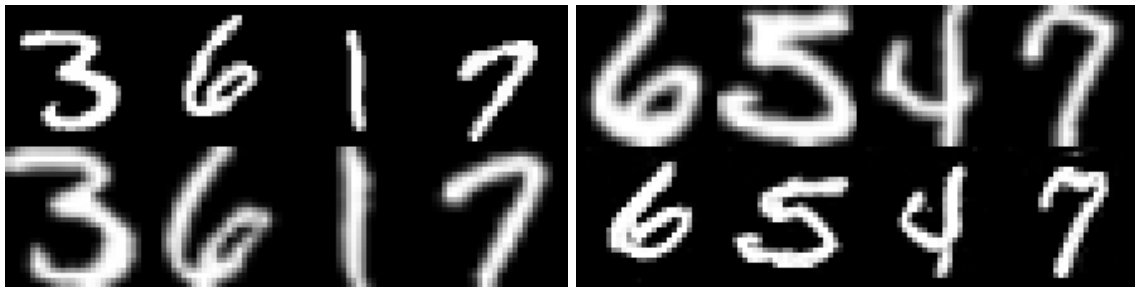
Table 2 reports our results on the evaluation settings. SBADA-GAN proves to be extremely effective, obtaining the new SOTA in all cases but *SVHN -> MNIST*, where we are on par with [28], which share our same classifier architecture but with 5x times the number of FC neurons, while [24] [10] use deeper classifiers with more convolutional layers. For all other experiments the improvement in performance is sizable, with a peak in the *MNIST -> SVHN* of a +20% compared to the previous SOTA.

We explain the success of SBADA-GAN in several ways. To begin with, by mapping both the source to target, and vice versa, we avoid having to decide a priori which is the best strategy for a specific task. For instance, we see in table 2 that on *SVHN -> MNIST* *SBADA-GAN inverse* achieves better results than *SBADA-GAN direct*. Another important feature is that the combination of the two branches always improves performance (especially in the *MNIST -> SVHN* setting). This is empirical evidence that the two branches are learning different, complementary features. Furthermore, our class consistency loss, allowing both domain transfers to influence each other, seems to provide a serious benefit; in fact our architecture



(a) MNIST to MNIST-M

(b) MNIST-M to MNIST



(c) MNIST to USPS

(d) USPS to MNIST



(e) MNIST to SVHN

(f) SVHN to MNIST

Figure 3: Examples of generated digits: top row is original data, bottom row is generated output.

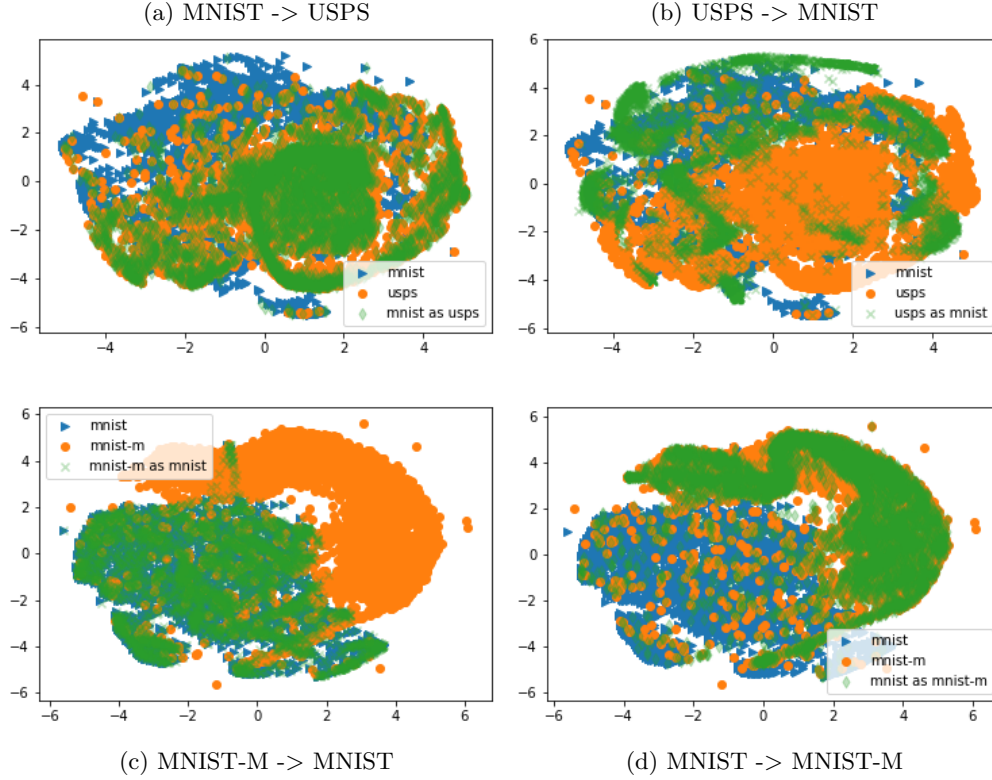


Figure 4: TSNE visualization of source, target and source mapped to target images. Note how the mapped source covers faithfully the target space.

	MNIST to USPS	USPS to MNIST	MNIST to MNISTM	SVHN to MNIST	MNIST to SVHN
Source Only	78.9	57.1 \pm 1.7	63.6(56.6)	60.1 \pm 1.1	26.0 \pm 1.2
CORAL[26]	81.7		57.7	63.1	
MMD [29]	81.1		76.9	71.1	
DANN [8]	85.1	73.0 \pm 2.0	77.4	73.9	
DSN [3]	91.3		83.2	82.7	
CoGAN [17]	91.2	89.1 \pm 0.8	62.0	no converge	
ADDA [28]	89.4 \pm 0.2	90.1 \pm 0.8		76.0 \pm 1.8	
GenToAdapt [24]	92.5 \pm 0.7	90.8 \pm 1.3		84.7 \pm 0.9	36.4 \pm 1.2
DRCN [10]	91.8 \pm 0.09	73.7 \pm 0.04		82.0 \pm 0.16	40.1 \pm 0.07
GOOGLE [2]	95.9	—	98.2		
Target Only	96.5		96.4(95.9)	99.5	
SBADA-GAN direct	96.66	94.43	99.13	72.20	59.21
SBADA-GAN inverse	97.10	87.47	98.37	74.2	50.85
SBADA-GAN	97.60	95.04	99.39	76.14	61.08

Table 2: Comparison of SBADA-GAN to the SOTA. *SBADA-GAN direct* is the setting where the target T is evaluated on the classifier trained in target space (C_{st}). *SBADA-GAN inverse* is the accuracy on target T , mapped to S , evaluated on the classifier trained in source space (C_{ts}). *SBADA-GAN* shows results obtained by a weighted (coefficients learned on the validation) linear combination of the softmax outputs of our two classifier. Note that all competitors convert SVHN to grayscale, while we are dealing with the more complex original RGB version.

is quite similar (minus this specific loss) to [2](in image space) and [28](in feature space) and, even in the simple *SBADA-GAN direct* setting, we outperform them.

5 Conclusion

This paper presented SBADA-GAN, an adaptive adversarial domain adaptation architecture that maps simultaneously source samples into the target domain and vice versa with the aim to learn and use both classifiers at test time. To achieve this, we proposed to use self-labeling to regularize the classifier trained on the source, and we impose a class consistency loss that improves greatly the stability of the architecture, as well as the quality of the reconstructed images in both domains. Qualitative and quantitative experiments confirm the power of our network. We plan to extend this work by investigating different schemes for taking advantage of the two classifiers of the system, and by testing it on other domain adaptation challenges, such as depth-to-RGB/ RGB-to-depth and synthetic-to-real settings.

Acknowledgments

This work was supported by the ERC grant 637076 - RoboExNovo.

References

- [1] P. Arbelaez, M. Maire, C. Fowlkes, and J. Malik. Contour detection and hierarchical image segmentation. *IEEE transactions on pattern analysis and machine intelligence*, 33(5):898–916, 2011.
- [2] K. Bousmalis, N. Silberman, D. Dohan, D. Erhan, and D. Krishnan. Unsupervised pixel-level domain adaptation with gans. In *Computer Vision and Pattern Recognition (CVPR)*, 2017.
- [3] K. Bousmalis, G. Trigeorgis, N. Silberman, D. Krishnan, and D. Erhan. Domain Separation Networks. In *Neural Information Processing Systems (NIPS)*, 2016.
- [4] F. M. Carlucci, L. Porzi, B. Caputo, E. Ricci, and S. R. Buló. Autodial: Automatic domain alignment layers. *Preprint arXiv:1704.08082*, 2017.
- [5] F. Chollet. keras. <https://github.com/fchollet/keras>, 2017.
- [6] J. Friedman, T. Hastie, and R. Tibshirani. *The elements of statistical learning*, volume 1. Springer series in statistics Springer, Berlin, 2001.
- [7] Y. Ganin and V. Lempitsky. Unsupervised domain adaptation by backpropagation. In *ICML*, 2015.
- [8] Y. Ganin, E. Ustinova, H. Ajakan, P. Germain, H. Larochelle, F. Laviolette, M. Marchand, and V. Lempitsky. Domain-adversarial training of neural networks. *J. Mach. Learn. Res.*, 17(1):2096–2030, 2016.
- [9] L. A. Gatys, A. S. Ecker, and M. Bethge. Image style transfer using convolutional neural networks. In *Conference on Computer Vision and Pattern Recognition (CVPR)*, 2016.
- [10] M. Ghifary, W. B. Kleijn, M. Zhang, D. Balduzzi, and W. Li. Deep reconstruction-classification networks for unsupervised domain adaptation. In B. Leibe, J. Matas, N. Sebe, and M. Welling, editors, *European Conference on Computer Vision (ECCV)*, 2016.
- [11] I. Goodfellow, J. Pouget-Abadie, M. Mirza, B. Xu, D. Warde-Farley, S. Ozair, A. Courville, and Y. Bengio. Generative adversarial nets. In *Neural Information Processing Systems (NIPS)*. 2014.

- [12] S. Ioffe and C. Szegedy. Batch normalization: Accelerating deep network training by reducing internal covariate shift. *arXiv preprint arXiv:1502.03167*, 2015.
- [13] J. Johnson, A. Alahi, and L. Fei-Fei. Perceptual losses for real-time style transfer and super-resolution. In *European Conference on Computer Vision (ECCV)*, 2016.
- [14] T. Kim, M. Cha, H. Kim, J. K. Lee, and J. Kim. Learning to discover cross-domain relations with generative adversarial networks. *Preprint arXiv:1703.05192*, 2017.
- [15] D. Kingma and J. Ba. Adam: A method for stochastic optimization. In *ICLR*, 2015.
- [16] Y. LeCun, L. Bottou, Y. Bengio, and P. Haffner. Gradient-based learning applied to document recognition. *Proceedings of the IEEE*, 86(11):2278–2324, 1998.
- [17] M.-Y. Liu and O. Tuzel. Coupled generative adversarial networks. In D. D. Lee, M. Sugiyama, U. V. Luxburg, I. Guyon, and R. Garnett, editors, *Neural Information Processing Systems (NIPS)*. 2016.
- [18] L. v. d. Maaten and G. Hinton. Visualizing data using t-sne. *Journal of Machine Learning Research*, 9(Nov):2579–2605, 2008.
- [19] X. Mao, Q. Li, H. Xie, R. Y. Lau, and Z. Wang. Multi-class generative adversarial networks with the l2 loss function. *arXiv preprint arXiv:1611.04076*, 2016.
- [20] M. Mirza and S. Osindero. Conditional generative adversarial nets. *Preprint arXiv:1411.1784*.
- [21] Y. Netzer, T. Wang, A. Coates, A. Bissacco, B. Wu, and A. Y. Ng. Reading digits in natural images with unsupervised feature learning. In *NIPS workshop on deep learning and unsupervised feature learning*, volume 2011, page 5, 2011.
- [22] A. Odena, C. Olah, and J. Shlens. Conditional image synthesis with auxiliary classifier gans. *arXiv preprint arXiv:1610.09585*, 2016.
- [23] T. Salimans, I. J. Goodfellow, W. Zaremba, V. Cheung, A. Radford, and X. Chen. Improved techniques for training gans. In *Neural Information Processing Systems (NIPS)*, 2016.
- [24] S. Sankaranarayanan, Y. Balaji, C. D. Castillo, and R. Chellappa. Generate to adapt: Aligning domains using generative adversarial networks. *arXiv preprint arXiv:1704.01705*, 2017.
- [25] A. Shrivastava, T. Pfister, O. Tuzel, J. Susskind, W. Wang, and R. Webb. Learning from simulated and unsupervised images through adversarial training. *Preprint arXiv:1612.07828*, 2016.
- [26] B. Sun, J. Feng, and K. Saenko. Return of frustratingly easy domain adaptation. In *AAAI*, 2016.
- [27] Y. Taigman, A. Polyak, and L. Wolf. Unsupervised cross-domain image generation. *International Conference on Learning Representations (ICLR)*, 2017.
- [28] E. Tzeng, J. Hoffman, T. Darrell, and K. Saenko. Adversarial discriminative domain adaptation. In *Computer Vision and Pattern Recognition (CVPR)*, 2017.
- [29] E. Tzeng, J. Hoffman, N. Zhang, K. Saenko, and T. Darrell. Deep domain confusion: Maximizing for domain invariance. *Preprint arXiv:1412.3474*, 2014.
- [30] J. Zhu, T. Park, P. Isola, and A. A. Efros. Unpaired image-to-image translation using cycle-consistent adversarial networks. *Preprint arXiv:1703.10593*, 2017.